

# Particle-Guided Image Registration

JooHWi Lee<sup>1</sup>, Ilwoo Lyu<sup>1</sup>, İpek Oğuz<sup>3</sup>, and Martin A. Styner<sup>1,2</sup>

<sup>1</sup> Department of Computer Science, University of North Carolina at Chapel Hill, Chapel Hill, NC 27514, USA

<sup>2</sup> Department of Psychiatry, School of Medicine, University of North Carolina at Chapel Hill, Chapel Hill, NC 27514, USA

<sup>3</sup> Electrical and Computer Engineering, The University of Iowa, Iowa City, IA 52246, USA

**Abstract.** We present a novel image registration method based on B-spline free-form deformation that simultaneously optimizes particle correspondence and image similarity metrics. Different from previous B-spline based registration methods optimized w.r.t. the control points, the deformation in our method is estimated from a set of dense unstructured pair of points, which we refer as *corresponding particles*. As intensity values are matched on the corresponding location, the registration performance is iteratively improved. Moreover, the use of corresponding particles naturally extends our method to a group-wise registration by computing a mean of particles. Motivated by a surface-based group-wise particle correspondence method, we developed a novel system that takes such particles to the image domain, while keeping the spirit of the method similar. The core algorithm both minimizes an entropy based group-wise correspondence metric as well as maximizes the space sampling of the particles. We demonstrate the results of our method in an application of rodent brain structure segmentation and show that our method provides better accuracy in two structures compared to other registration methods.

## 1 Introduction

The study of brain changes in rodent models of neuropathology and drug exposure has been of increasing interest to the neuroscience community. In contrary to human studies, rodent models have several advantages, such as a well controlled environments and access to genetic modifications as well as shorter lifespan. Magnetic Resonance Imaging (MRI) has emerged as an important modality to study such rodent brain morphological changes. Non-rigid registration is a crucial tool to process such MRIs providing structural segmentations and enabling the analysis of group differences.

Several methods have been proposed for the study of rodent brains. Among those atlas-based registration methods are popularly used. However, a single atlas-based method has a disadvantage of the introduction of bias that might cause poor segmentation and dilute the difference between groups [6]. Group-wise registration method which deals with every subject together can be an

alternative to reduce the effects of template selection [2]. Since a group-wise registration method does not require the choice of a template or reference, it is expected to produce consistent results which means a consistent comparison of groups.

Motivated by a particle correspondence algorithm [3], a non-parametric and group-wise surface correspondence method, we propose a novel group-wise image registration method guided by particles. These particles are distributed inside a particular region and directly optimized so that each particle will be placed at corresponding positions across subjects minimizing a group-wise intensity metric. During this optimization, a B-spline free-form deformation is estimated for each subject to constitute a common reference frame. The contributions of the proposed method are following:

1. **Unbiased Group-Wise Registration with Implicit Mean:** Instead of choosing a specific template, a common reference frame is estimated from dynamic particles distributed inside ROIs, *i.e.* a brain mask. Using the Euclidean mean of those particles, each subject is efficiently registered into a common space.
2. **Computational Efficiency with Particles:** Since the number of particles is fewer than the number of voxels, a common reference frame is more efficiently computed than other methods [2]. We compensate this sparsity by considering a local patch for each particle, which also provides robust performance than single voxel random sampling strategy.
3. **Flexibility in Adaptive Processing:** In contrary to a regular control point grid, particles are unstructured and independent each other so that it is easy to adopt adaptive strategy depending on local context. For example, particles can be easily placed more densely in salient areas, *i.e.* edges, by controlling a single parameter.

As our work is in an early stage, we demonstrate preliminary results of rodent brain structure segmentation with comparison to two different registration methods for humans: the spline-based FFD available in Slicer and to SyN available in ANTS. We show that our group-wise algorithm performs better in different sizes as well as produces statistically indifferent results with the comparing methods otherwise.

## 2 Methods

We propose a group-wise image registration method guided by dynamic particles. The structure of our method is similar to the surface-based particle correspondence algorithm [3] and can be thought as an extension of the algorithm. The application of particles in an image domain, however, has never been attempted. Our method is also uniquely different from the previous one in that we introduce B-spline free-form deformation to associate different subject spaces as well as deal with local patch information for robust performance.

## 2.1 Particle Correspondence with Local Similarity

The main goal of our method is to drive each particle toward a corresponding position that satisfies two conditions in the mean space: 1) overlapping of particles and 2) local intensity similarity. The particles are governed by two forces: a positional coherence force and a force from local intensity similarity.

To describe the motion of particles, we define the particle system  $\mathbf{P}$  that comprises  $N$  number of subject volumes  $\mathbf{V} = \{V^1, V^2, \dots, V^N\}$ . For each subject  $j$ , we sample the same  $n$  number of particles  $P^j = \{p_1^j, p_2^j, \dots, p_n^j\}$  in which  $p_i = \{p_i^1, p_i^2, \dots, p_i^N\}$  is the corresponding particles from each subject. From these correspondences, an implicit mean space  $\bar{V}$  is estimated from the mean of particles  $\bar{P} = \frac{1}{N} \sum_{j=1}^N P^j$ . Our group-wise registration process is formulated to find an optimal particle configuration  $\check{p}_i^j$  that minimizes a positional coherence metric  $H_P(p_i)$  and a local intensity similarity metric  $H_I(p_i)$ . The final dense deformation field  $\check{T}_j$  that maps  $V^j$  to  $\bar{V}$  is derived by taking  $P^j$  and  $\bar{P}$  as a set of correspondences.

**Correspondence Formulation.** By the transform  $T_j$ , a particle  $p_i^j$  is mapped to  $q_i^j \in \bar{V}$ . Ideally, it is assumed that  $q_i^1 \simeq q_i^2 \simeq \dots \simeq q_i^N$ . Therefore, each particle of  $p_i$  should move to the direction where the variance of  $q_i$  is minimized as depicted in Figure 1a. In the mean time, if there is local differences in intensity values, the particles are allowed to deviate from the overlapping position so that the local variance of intensity values are minimized such that  $I^1(q_i^1) \simeq I^2(q_i^2) \simeq \dots \simeq I^N(q_i^N)$  where  $I^j = V_j(T_j^{-1}(q_i))$ . To compare similarity among a group, [3] and [2] approach in similar using entropy. The entropy of a random variable  $q$  with a given p.d.f  $f(q)$  is minimized when there is less information in  $q$  and formulated  $H(q) = -\int f(q) \log(f(q)) dq$ . Denoting the random variable as  $q_i$  and  $\mathcal{I}_i$  respectively for  $q_i^j$  and  $I^j(q_i^j)$ , the goal is to find the optimal particle configuration  $\hat{\mathbf{P}}$  such that

$$\hat{\mathbf{P}} = \arg \min_{P^j \in \Omega_j} S(P) = \lambda_P \sum_{i=1}^n H_P(q_i) + \lambda_I \sum_{i=1}^n H_I(\mathcal{I}_i). \quad (1)$$

Since the number of particles is much smaller than the number of voxels, we sample a local patch near by a particle  $q_i^j$  so that  $\mathcal{I}_i^j = \{I_i^j(1), I_i^j(2), \dots, I_i^j(M)\}$ , where  $M$  is the number of neighborhoods of  $q_i^j$ .

**Correspondence Optimization.** Given covariance matrices of  $\Sigma$  and  $\Lambda$  that follows  $N$ , we derive  $H_P$  and  $H_I$  analytically [7] so that

$$H_P(q_i) = -r + \frac{1}{2} \ln(2\pi)^r |\Sigma|, \quad H_I(\mathcal{I}_i) = -M + \frac{1}{2} \ln(2\pi)^M |\Lambda|, \quad (2)$$

where  $r$  is the dimension of  $q$  and  $|\Sigma|$  and  $|\Lambda|$  are the determinants. The gradient of  $H_P$  and  $H_I$  in the space of  $V$  are given  $\frac{\partial H_P}{\partial p} = \mathbf{J}_{T_j^{-1}} \check{p}^j (\Sigma + \alpha I)^{-1}$  and

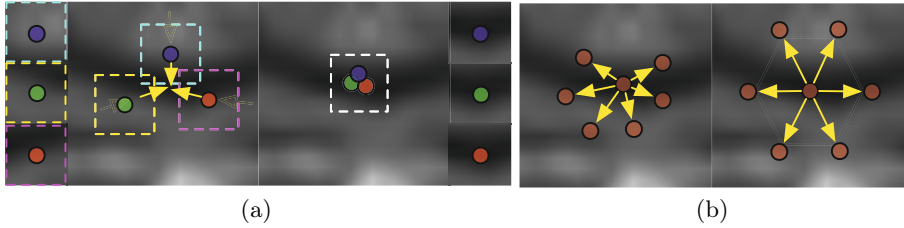


**Fig. 1.** Schematic diagram of (a) overlapping particles and local intensity similarity in correspondence across subjects. Colored in blue, green, and red, each particle has correspondence across subjects and attracts together minimizing  $H_P$ . At the same time, the entropy of local intensities sampled in colored squares is also minimized so that the particles stay at a locally similar position. (b) a repulsion force uniformly distributes in-subject particles to fill a given region.

$\frac{\partial H_I}{\partial p} = \mathbf{J}_{T_j^{-1}} I' (\Lambda + \beta)^{-1} \frac{\partial I}{\partial p}$ , respectively. where  $\tilde{p}'$  and  $I'$  are displacement from the mean and  $\alpha, \beta$  is a relaxation factor to avoid degenerative cases.

From the particle perspective, the negative gradient direction,  $-\frac{\partial H_P}{\partial p}$  and  $-\frac{\partial H_I}{\partial p}$  can be interpreted as two different forces: a positional coherence force and an intensity force as depicted in Fig. 1.

## 2.2 Particle Sampling in a Volume

Corresponding particles across subjects are attracted together to be overlapped at a locally similar position. Without an appropriate repulsion force, the particles would degenerate to a single point. Moreover, since we sample local intensity values nearby a particle, a repulsion force is required to uniformly sample a given image domain. In order for that, we extend the surface-based particle correspondence algorithm [3] to the image domain to uniformly sample a set of particles in a volume. In the algorithm, each particle position is rendered as a random variable with regard to a particular region and iteratively optimized to maximally contain the spatial information of the region.

**Problem Definition.** Given a bounded region of interest  $\Omega$  in a volume  $V$ , we sample  $n$  number of points  $X = (x_1^T, x_2^T, \dots, x_n^T)^T \in \Omega^n$  where  $x_i = (x, y, z)$ . By letting  $\mathcal{X}$  be a random variable of  $X$ , the goal is to find an instance  $\tilde{X}$  such that

$$\tilde{X} = \arg \max_{\tilde{X} \in \Omega^n} H_S[\mathcal{X}] = \arg \min_{\tilde{X} \in \Omega^n} \sum_{i=1}^n \int_{x_i \in \Omega} p(x_i) \log p(x_i) dx_i, \quad (3)$$

where  $H_S$  is the differential entropy

$$H_S(\mathcal{X}) = - \int_{X \in \Omega^n} p(X) \log p(X) dX, \quad (4)$$

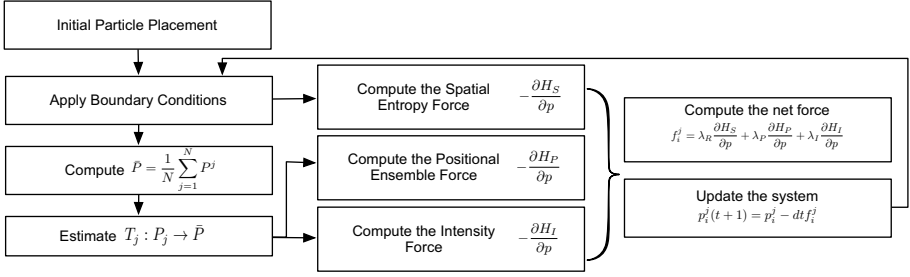


**Fig. 2.** Overall algorithm flow. The registration process is finished when the system stabilizes, and images are registered with the estimated  $T_j$ .

and  $p(X)$  is the p.d.f of  $X$ . Assuming  $x_i$  is i.i.d,  $H_S(\mathcal{X})$  can be decomposed into the sum of the spatial entropy  $H_S(x_i)$ . From the definition,  $\tilde{X}$  contains maximal information of  $\Omega$ .

**Sampling Optimization.** A key step to compute  $H_S[\mathcal{X}]$  is the density estimation of  $p(x)$ . The density for a particle is estimated as  $p(x_i) = \frac{1}{n(n-1)} \sum_{j=1, j \neq i}^n G(x_i - x_j, \sigma_i)$  using a nonparametric, Parzen windowing estimation[3] with the assumption of Gaussian. The negative gradient of  $H_S[\mathcal{X}]$  to maximize the cost function is

$$-\frac{\partial H_S}{\partial x_i} = \frac{1}{\sigma_i^2} \frac{\sum_{j \neq i}^n (x_i - x_j) G(x_i - x_j, \sigma_j)}{\sum_{j \neq i}^n G(x_i - x_j, \sigma_j)} = \sigma_i^{-2} \sum_{j \neq i}^n (x_i - x_j) w_{ij}. \quad (5)$$

For the optimization, we employ a standard gradient descent optimization via Euler scheme,  $x_{t+1} = x_t - \alpha \frac{\partial H_S}{\partial x}$ . The control of adaptivity is achieved by assigning different  $\sigma_j$  for each particle [5].

### 2.3 B-spline Deformation Driven by Corresponding Particles

An improved FFD B-spline is proposed by [9]. In [9], the authors show that the straightforward optimization of B-spline control points is suboptimal and propose a fitting-based strategy that directly manipulates free-form deformations. In the same regard, we estimate the deformation  $T_j$  directly from the set of corresponding particles interpolating B-spline deformation in Least Squares sense. [8] gives a solution for the interpolation generalized to  $n$ -dimensional scattered data. The overall algorithm flow of our method is shown in Fig. 2.

### 2.4 Particle Initialization

Since the registration is performed by iterative particle optimization, the initial particle placement is important to achieve good registration results. Assuming that a basic preprocessing such as the rigid or affine registration is performed, we compute the initial particle placement as following:

1. Compute the intersection  $\Omega_M$  of a set of given ROIs  $\Omega_1, \Omega_2, \dots, \Omega_N$
2. Choose random particle samples  $\mathbf{X}$ , inside of the intersection  $\Omega_M$
3. Uniformly distribute the sampled particles  $\mathbf{X}$  inside  $\Omega_M$
4. Transfer  $\mathbf{X}$  into each subject  $i$  and distribute  $\mathbf{X}_i$  inside  $\Omega_i$

We rely on this heuristic to set up particles. By gradually distributing particles, the corresponding particles will be located at similar position inside each mask  $\Omega$ . This strategy is specifically useful for rodent brain where the volume of each subcortical structure is proportional to whole brain.

### 3 Experimental Results

#### 3.1 Data Set

The data set acquired post mortem, at 3 age groups across adolescence (postnatal days 28 through 80). MR images of each animal using a Bruker BioSpec 9.4T horizontal bore MRI system (Bruker, Billerica, MA). Images were acquired using a 4-channel phase-array surface coil with the rat in supine position. 3D MDEFT sequence was used for T1-weighted image acquisition with the following parameters: TE=6.7 ms, TR=4000 ms, NEX=4; matrix size of  $320 \times 210$ , and the voxel size of 0.1mm isotropic, and acquisition time was 6 hours. To improve signal-to-noise-ratio (SNR), two images were acquired immediately following each other for each animal, and these two were averaged together following rigid registration. Total imaging time was 12 hours.

#### 3.2 Evaluation

For the preliminary results of our method, we compared the results of our method with two popularly used non-rigid registration methods using cross correlation as a similarity metric: the non-rigid FFD B-spline image registration method packaged in Slicer3, and the SyN image registration method implemented in ANTS [1]. To study the performance of our group-wise registration, we warped manual regions of interests of brain structures, Thalamus and Cerebellum, of each subject to every other subject with each method. We included all 17 subjects ranging from postnatal days 28 to postnatal days 72 and computed total 272 pairs. We then computed Dice overlap ratios ( $2|A \cap B|/(|A| + |B|)$ ) between the manual and automatic structural segmentations. For the proposed method, we sampled 2048 particles from each volume and used  $7 \times 7 \times 7$  intensity regions per each particle. For B-spline displacement field interpolation, we used  $8 \times 8 \times 8$  control points grid with the order of 3 splines. Each compared method was applied with its default settings except the number of B-spline control points matched with ours. The average Dice ratios of two ROIs for post-mortem rat images for each method are shown in Table 1.

From the results, the proposed method showed higher Dice coefficients than other two methods. Our method showed better performance in Dice coefficients than the FFD B-spline implementation and ANTS tool in the manually segmented regions.

**Table 1.** Overall Dice coefficients and its standard deviation of Thalamus and Cerebellum, by the proposed group-wise method, Symmetric Diffeomorphic Mapping in ANTS, and FFD B-spline registration

Methods	Thalamus	Cerebellum
The proposed method	86% ( $\pm 8\%$ )	87.8% ( $\pm 6\%$ )
ANTS	81% ( $\pm 6\%$ )	84% ( $\pm 14\%$ )
B-spline	81% ( $\pm 6\%$ )	79% ( $\pm 11\%$ )

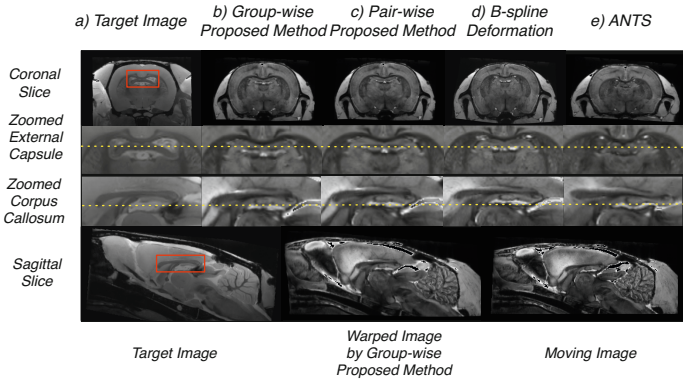


**Fig. 3.** Visual comparison of segmentation results. From left to right, the moving, fixed, result of proposed method, B-spline, and ANTS respectively in the first three rows. The bottom row shows sagittal slices of the fixed image, the result of the proposed image, and the moving image. The intensity scale was inverted during the acquisition but corrected in the experiments.

## 4 Conclusion

We proposed a novel image registration method that is guided by dynamic particles. Having correspondences each other, those particles are driven to locally similar positions in the mean space. By computing an implicit mean rather than an explicit image, our method was efficiently performed group-wise image registration in a linear time with respect to the number of subjects. Our method can be immediately applied to for example the multi-atlas joint registration/segmentation, the detection of outliers in a large data study, the inclusion of statistical shape information during registration, etc. Since the proposed method stays at a very early stage of research, future work will include thorough validation for its accuracy and robustness as well as comparison to other group-wise registration method [2,4,10].

**Acknowledgements.** The following grants are acknowledged for financial support: P01 DA022446, P30 HD03110, R41 NS059095, U01 AA020022, A020023, A020024, AA06059, AA019969, U54 sEB005149.

## References

1. Avants, B.B., Epstein, C.L., Grossman, M., Gee, J.C.: Symmetric diffeomorphic image registration with cross-correlation: Evaluating automated labeling of elderly and neurodegenerative brain. *Medical Image Analysis* 12(1), 26–41 (2008)
2. Balci, S.K., Golland, P., Shenton, M., Wells, W.M.: Free-form b-spline deformation model for groupwise registration. In: *Medical Image Computing and Computer-Assisted Intervention: MICCAI... International Conference on Medical Image Computing and Computer-Assisted Intervention*, vol. 10, p. 23. NIH Public Access (2007)
3. Cates, J.E., Fletcher, P.T., Styner, M.A., Shenton, M.E., Whitaker, R.T.: Shape modeling and analysis with entropy-based particle systems. In: Karssemeijer, N., Lelieveldt, B. (eds.) *IPMI 2007. LNCS*, vol. 4584, pp. 333–345. Springer, Heidelberg (2007)
4. Joshi, S., Davis, B., Jomier, M., Gerig, G., et al.: Unbiased diffeomorphic atlas construction for computational anatomy. *NeuroImage* 23(1), 151 (2004)
5. Meyer, M.D., Georgel, P., Whitaker, R.T.: Robust particle systems for curvature dependent sampling of implicit surfaces. In: *2005 International Conference on Shape Modeling and Applications*, pp. 124–133. IEEE (2005)
6. Nie, J., Shen, D.: Automated segmentation of mouse brain images using multi-atlas multi-roI deformation and label fusion. *Neuroinformatics*, 1–11 (2013)
7. Oguz, I., Niethammer, M., Cates, J., Whitaker, R., Fletcher, T., Vachet, C., Styner, M.: Cortical correspondence with probabilistic fiber connectivity. In: Prince, J.L., Pham, D.L., Myers, K.J. (eds.) *IPMI 2009. LNCS*, vol. 5636, pp. 651–663. Springer, Heidelberg (2009)
8. Tustison, N.J., Gee, J.C.: Generalized  $n$ -D  $C^k$  B-spline scattered data approximation with confidence values. In: Yang, G.Z., Jiang, T.-Z., Shen, D., Gu, L., Yang, J. (eds.) *MIAR 2006. LNCS*, vol. 4091, pp. 76–83. Springer, Heidelberg (2006)
9. Tustison, N.J., Avants, B.A., Gee, J.C.: Improved ffd b-spline image registration. In: *IEEE 11th International Conference on Computer Vision, ICCV 2007*, pp. 1–8. IEEE (2007)
10. Wu, G., Yap, P.-T., Wang, Q., Shen, D.: Groupwise registration from exemplar to group mean: extending hammer to groupwise registration. In: *2010 IEEE International Symposium on Biomedical Imaging: From Nano to Macro*, pp. 396–399. IEEE (2010)